Supporting Information for

Optimize Hydrophobic Nanoparticles to Better Target Lipid Rafts with Molecular Dynamics Simulations

Xiaoqian Lin[1,2], Xubo Lin[1,2,*], Ning Gu[3,*]

1. Institute of Nanotechnology for Single Cell Analysis (INSCA), Beijing Advanced Innovation Center for Biomedical Engineering, Beihang University, Beijing 100191, China.
2. School of Biological Science and Medical Engineering, Beihang University, Beijing 100191, China.
3. State Key Laboratory of Bioelectronics, Jiangsu Key Laboratory for Biomaterials and Devices, School of Biological Sciences & Medical Engineering, Southeast University, Nanjing 210096, China

*Correspondence to linxbseu@buaa.edu.cn (XL) and guning@seu.edu.cn (NG)

1. Encapsulation of Hydrophobic NPs Shows Little Effects on the Lipid Raft Dynamics.

As shown in **Fig. S1**, we compared the normalized lateral contact N of unsaturated lipids for NP-embedded lipid membrane systems with the NP-free membrane system. The results indicated that the phase separation processes of DPPC/DUPC/Chol bilayers are not significantly affected by these ultra-small hydrophobic NPs. The lipid membrane can phase separate into stable raft and non-raft domains within the first 2 μs CGMD simulations. We also analyzed lipid chain order parameters (**Fig. S2**) and cholesterol preferences (**Fig. S3**) in these systems, which are tightly correlated with the lipid raft dynamics.

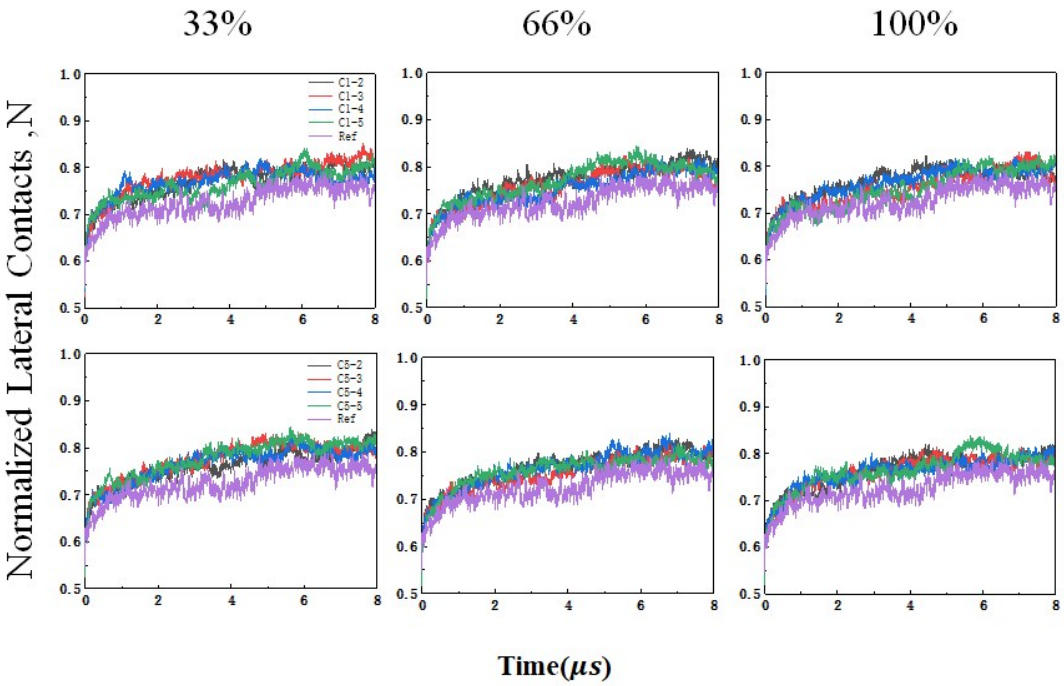

Figure S1. Time evolution of normalized lateral contact N of unsaturated lipids for NP-embedded lipid membrane systems (Ligand hydrophobicity: C1/C5, ligand length: nl=2, 3, 4, 5, ligand density: 33%, 66%, 100%) and the NP-free membrane system (Ref).

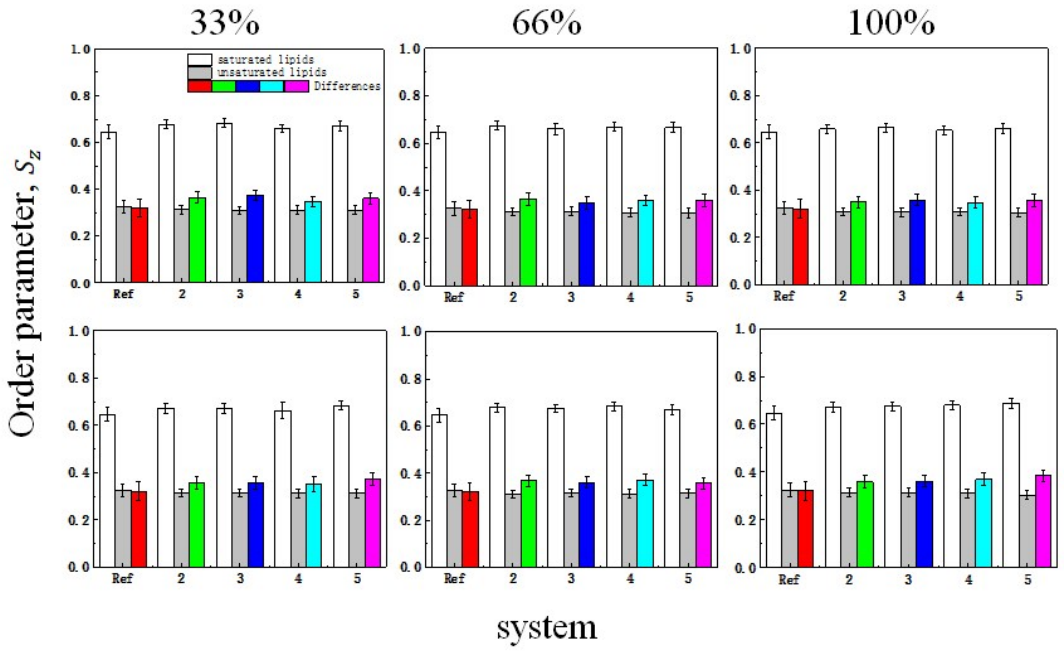

Figure S2. Lipid chain order parameter for NP-embedded lipid membrane systems (Ligand hydrophobicity: C1/C5, ligand length: nl=2, 3, 4, 5, ligand density: 33%, 66%, 100%) and the NP-free membrane system (Ref). The upper row shows the system with more hydrophobic NP ("C1"), and the lower row shows the system with less hydrophobic NP ("C5"). System 2-5 represent system with the ligand lengths of 2-5.

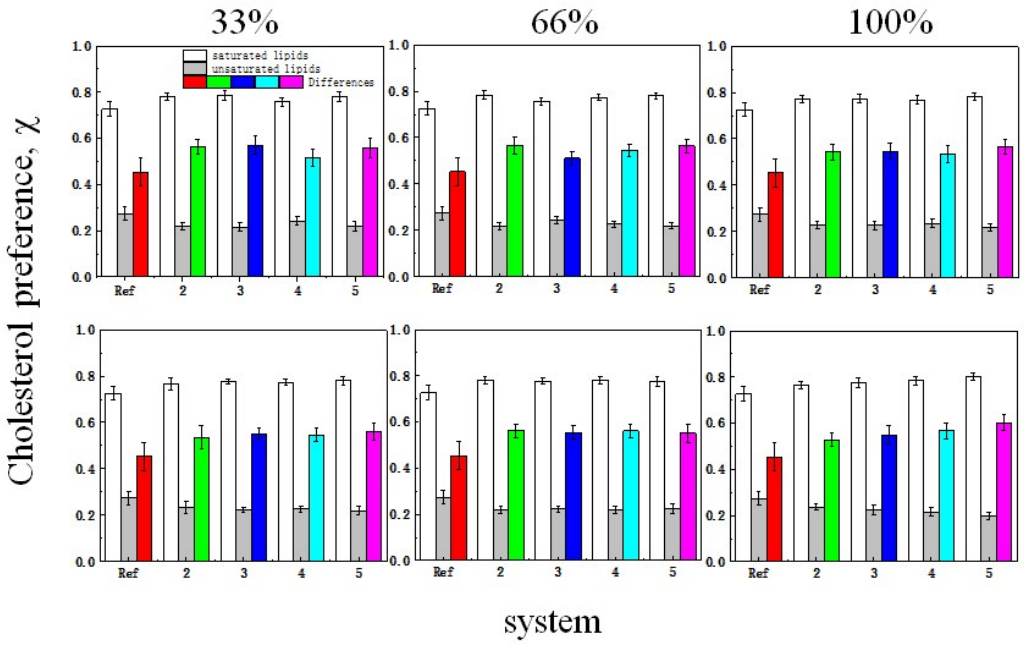

Figure S3. Percentage contact with cholesterol, χ, of saturated lipids, unsaturated lipids, and their differences for NP-embedded lipid membrane systems (Ligand hydrophobicity: C1/C5, ligand length: nl=2, 3, 4, 5, ligand density: 33%, 66%, 100%) and the NP-free membrane system (Ref). The upper row shows the system with more hydrophobic NP ("C1"), and the lower row shows the system with less hydrophobic NP ("C5"). System 2-5 represent system with the ligand lengths of 2-5.

2. Effects of the Ligand Hydrophobicity, Length and Density on the Partitioning Dynamics of NPs in Phase-separated Lipid Membranes.

In order to validate the results presented in the manuscript, we visualized system snapshots of the last frames of all simulations (**Fig. S4**) and performed 2D number-density maps analysis for each system. For less hydrophobic NPs ("C5"), no matter how you change the ligand density and length, NPs are always located in the non-raft domains **(Fig. S6)**. However, for more hydrophobic NPs ("C1"), the ligand density and length can affect NPs' membrane partitioning dynamics (**Fig. S5**). What's more, for the short ligand, reducing the ligand density will gradually shift the raft-preference of more hydrophobic ligand-modified NPs to the non-raft domain (**Fig. S6**). As shown in **Fig. S7**, the encapsulation of the NP did not significantly change the thickness of either raft or non-raft membrane domains. However, the ligand length and density jointly determined the local membrane thickness disturbance. For the case of the high ligand density and long ligand, the membrane thickness of the local area around the embedded NP is greatly increased. The effect of the ligand density is much more obvious than that of the ligand length. Both the two factors jointly determine the actual size of the embedded NP, and thus the local membrane thickness disturbance.

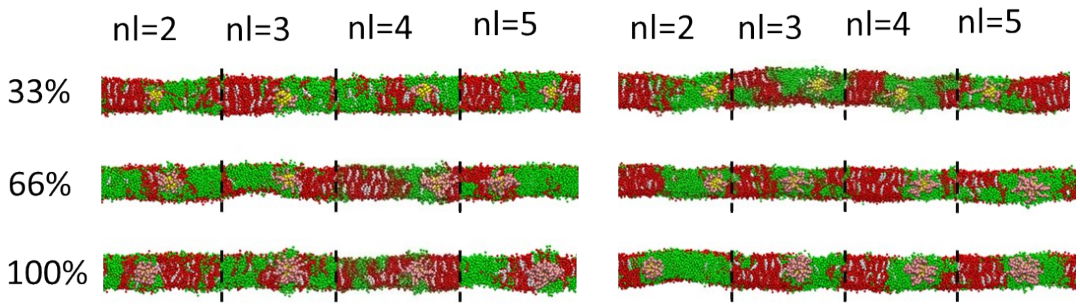

Figure S4. Effects of ligand hydrophobicity (C1/C5), length (nl=2, 3, 4, 5) and density (ligand density: 33%, 66%, 100%) on the membrane partitioning dynamics of ligand-modified NPs. The left one shows the system with more hydrophobic NP ("C1"), and the right one shows the system with less hydrophobic NP ("C5"). DPPC is colored in red, DUPC in green, CHOL in white, NP core in yellow, ligand in pink.

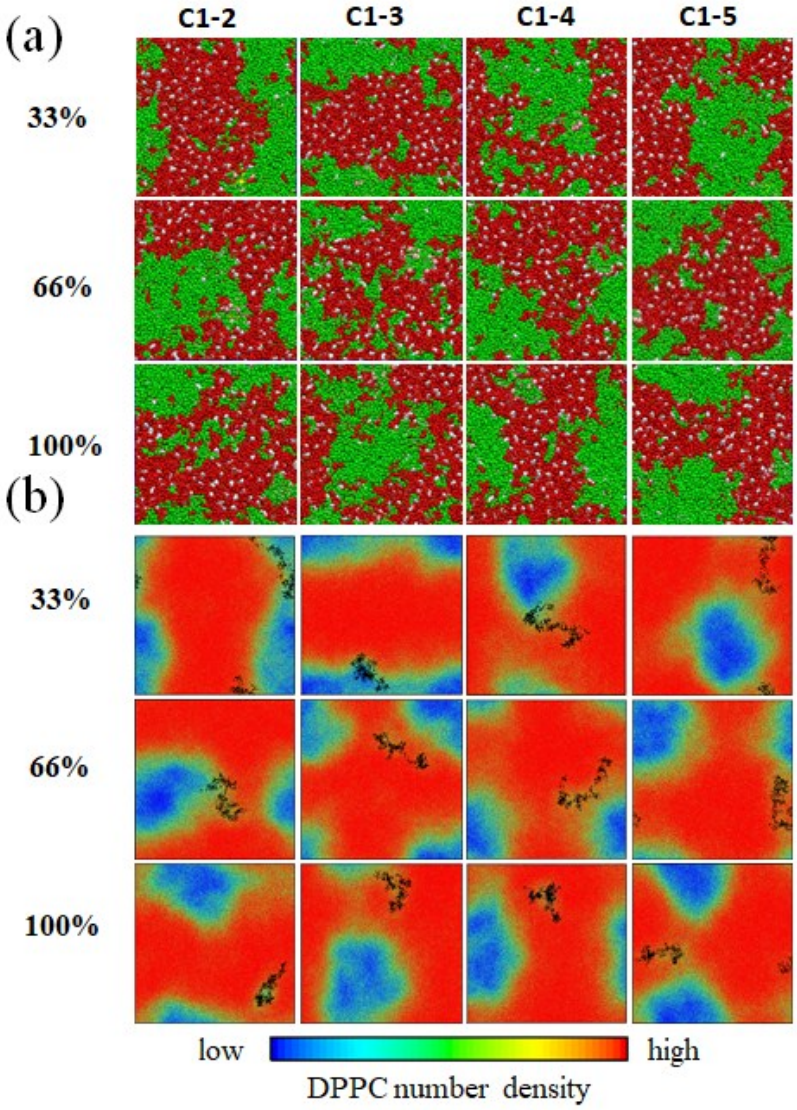

Figure S5. Effects of ligand density (33%, 66%, 100%) on the membrane partitioning dynamics of ligand-modified NPs (ligand hydrophobicity: C1, nl=2, 3, 4, 5). **(a)** Top-view system snapshots of the last frame of each 8 μs trajectory. **(b)** 2D number-density maps and the instantaneous location of NP (black points)

derived from analysis of each of the last 2 μs trajectories. The coloring style is the same as in **Fig. S4**.

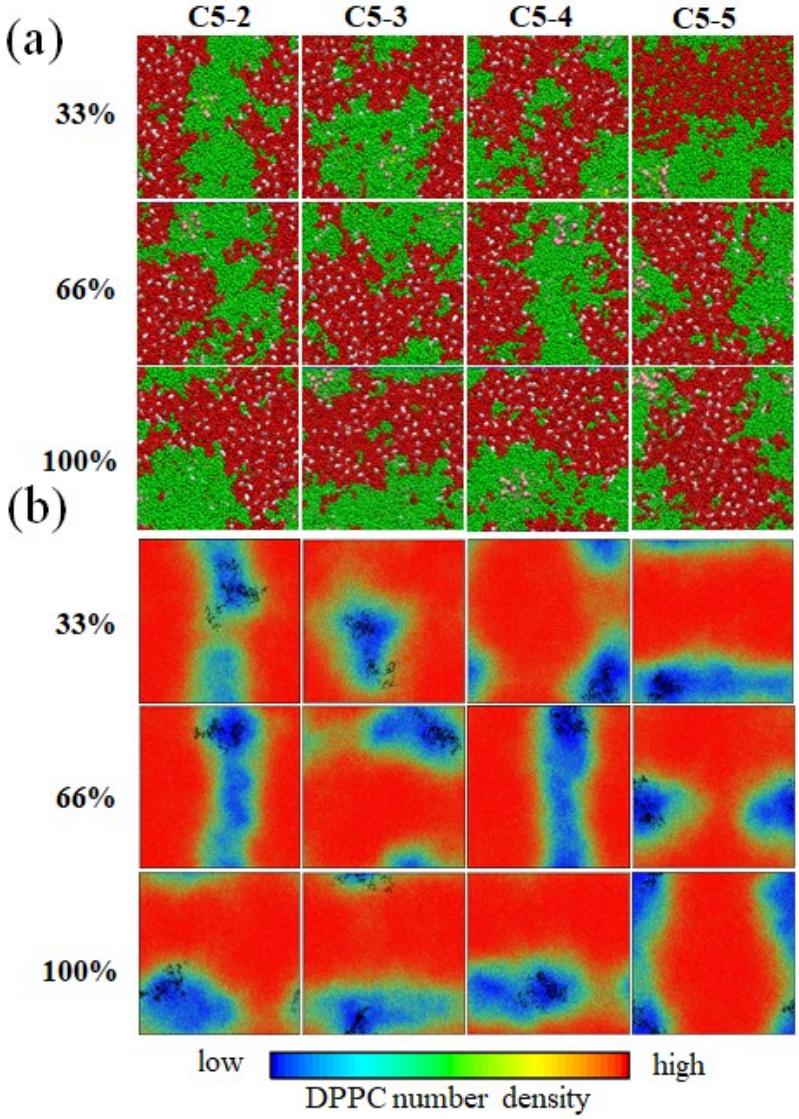

Figure S6. Effects of ligand density (33%, 66%, 100%) on the membrane partitioning dynamics of ligand-modified NPs (ligand hydrophobicity: C5, nl=2, 3, 4, 5). **(a)** Top-view system snapshots of the last frame of each 8 μs trajectory. **(b)** 2D number-density maps and the instantaneous location of NP (black points) derived from analysis of each of the last 2 μs trajectories. The coloring style is the same as in **Fig. S4.**

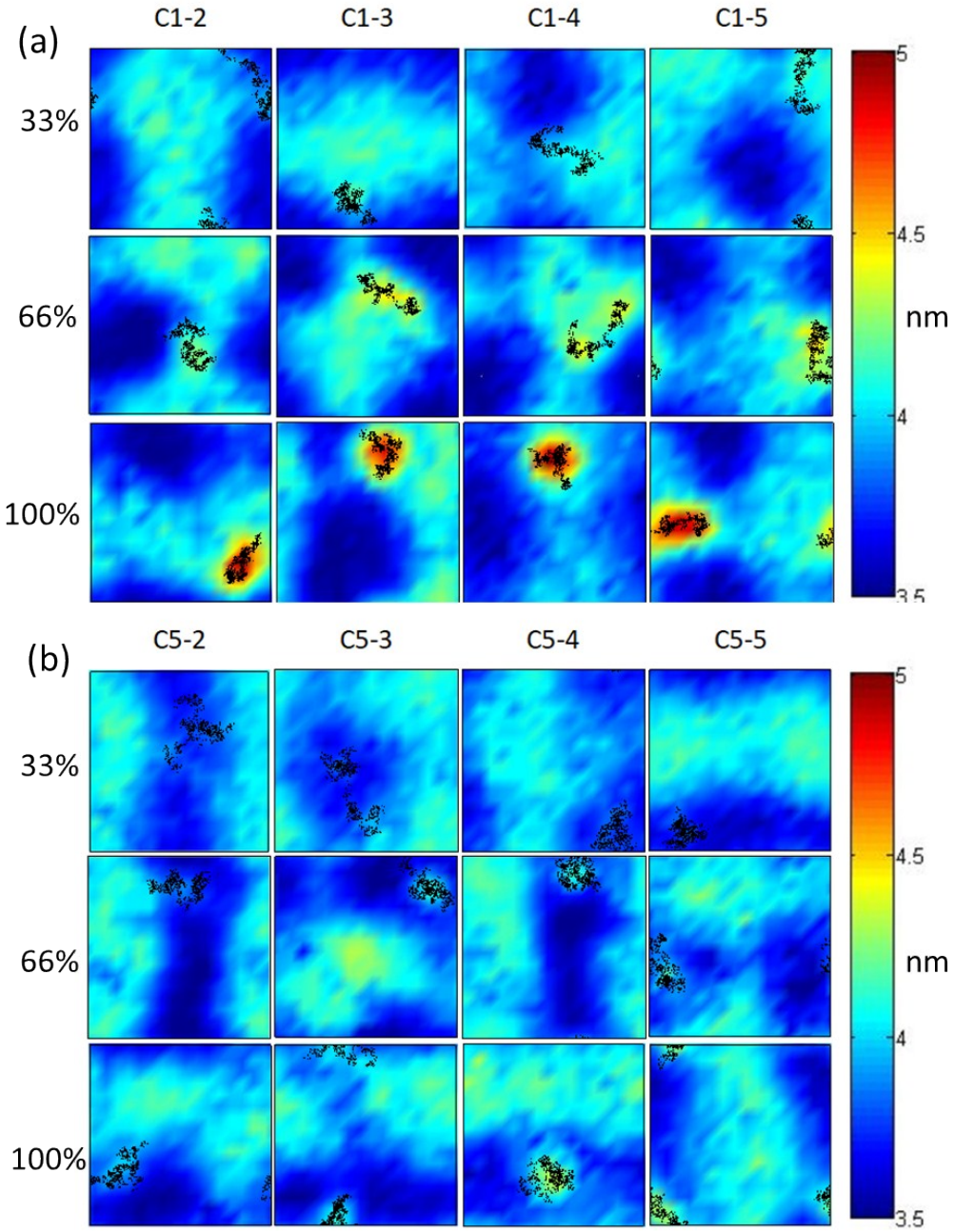

Figure S7. 2D Local membrane thickness distributions for all simulation systems (ligand hydrophobicity: C1/C5, ligand density: 33%, 66%, 100%, ligand length: nl=2, 3, 4, 5) and the corresponding NPs' trajectories (black points) averaged over the last 2 μs. The black point corresponds to the NP's trajectory projected in the x−y plane.

3. Local Disturbance of Embedded NPs on the Phase-separated Lipid Membranes.

In order to further validate the results shown in **Fig. 4** and **5**, the same analysis was performed for systems with different NPs (**Fig. S8** and **S9**).

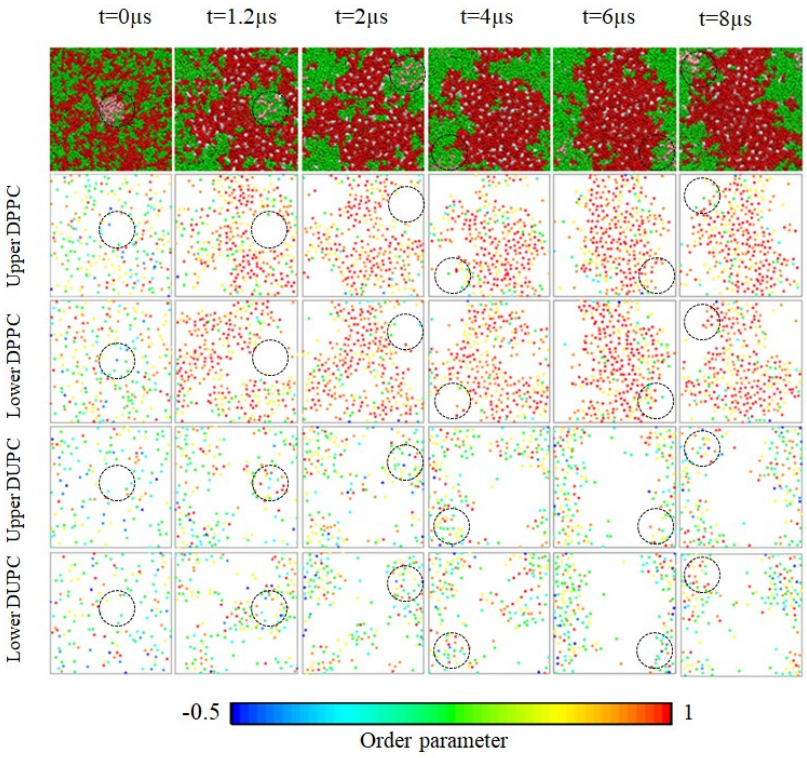

Figure S8. Time evolution of lipid order parameters for each lipid of NP-embedded lipid membrane systems (Ligand hydrophobicity: C5, ligand length: nl=5, ligand density: 100%). Each point represents one DPPC/DUPC molecule, and its color shows the averaged chain order parameters. The dashed black circle indicates the localization of the ligand-modified NP. The coloring style is the same as in **Fig. S4.**

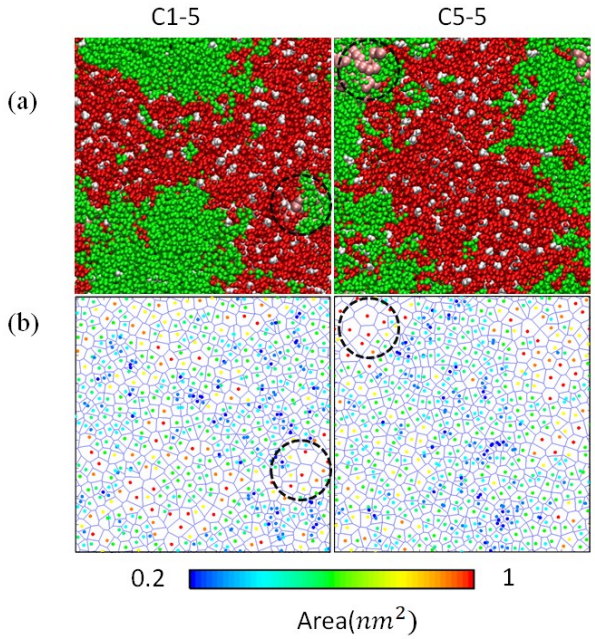

Figure S9. The encapsulation of ligand-modified NPs affects the local area per lipid. **(a)** Top-view system snapshots at the end of 8 μs CGMD simulations (Ligand hydrophobicity: C1/C5, ligand length: nl=4, ligand density: 100%). **(b)** Voronoi tessellation analysis of lipids in one monolayer at the end of 8 μs trajectories. The dots, which are colored with area per lipid, denote the center-of-mass of the DPPC/DUPC/CHOL groups. The coloring style is the same as in **Fig. S4.**

4. Effects of the Temperature on the Partitioning Dynamics of NPs in Phase-separated Lipid Membranes.

Since MD simulations of model membrane systems at T=298 K were widely validated in comparable in vitro experiments at room temperature, we chose 298 K (room temperature) for our MD simulations. In order to clarify the possible effects of the temperature on our main conclusion, several new coarse-grained MD simulations using 310 K have been performed (**Fig. S10**). When the temperature changes from 298 K to 310 K, the stability of the phase-separated membrane decreases (**Fig. S10c**). However, it has no obvious effect on the nanoparticles' (NPs') ultimate preferences to the lipid raft or non-lipid raft domains. The system snapshots (**Fig. S10a**) and 2D number-density maps (**Fig. S10b**) clearly indicated that more hydrophobic NPs (type "C1") tended to reside in the raft domain, while less hydrophobic NPs (type "C5") preferred the non-raft domain, which is exactly the same as the systems with a temperature of 298 K.

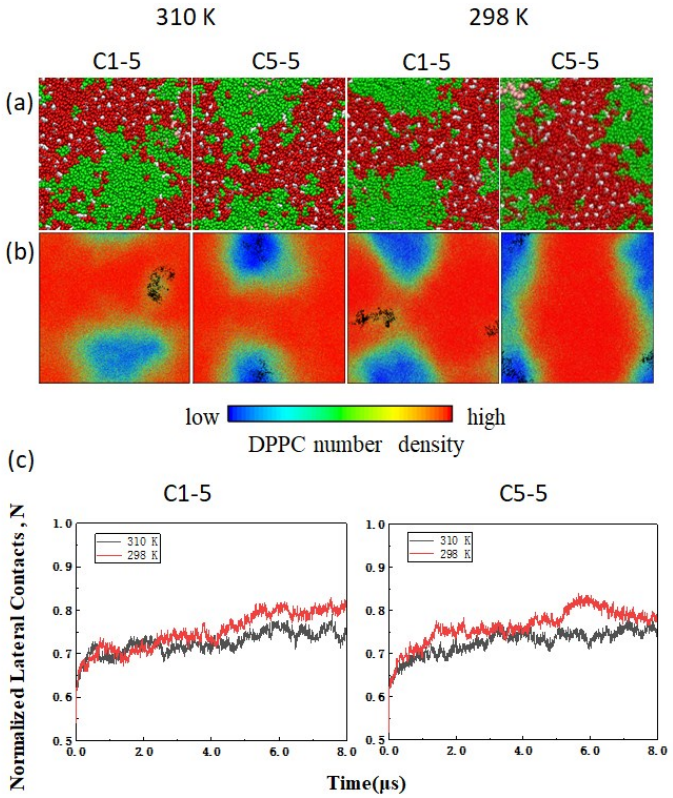

Figure S10. Effects of temperature on the membrane partitioning thermodynamics of ligand-modified NPs (ligand hydrophobicity: C1/C5, ligand density: 100%, ligand length: nl=5). **(a)** Top-view system snapshots of the last frame of each 8 μs trajectory. **(b)** 2D DPPC number-density maps and the NPs' localization (black points) over each of the last 2 μs trajectories. **(c)** Time evolution of normalized lateral contact N of unsaturated lipids. The coloring style is the same as in **Fig. S4**.

5. Nanoparticle Affects the Diffusion of the Raft as a Whole Entity.

The ligand-modified NPs were embedded in the phase separated membrane, which hardly affect the diffusion coefficients of either saturated (DPPC) or unsaturated lipids (DUPC) as shown in **Fig. S11**. This is also consistent with the results in the manuscript that these NPs do

not significantly affect the lipid raft dynamics.

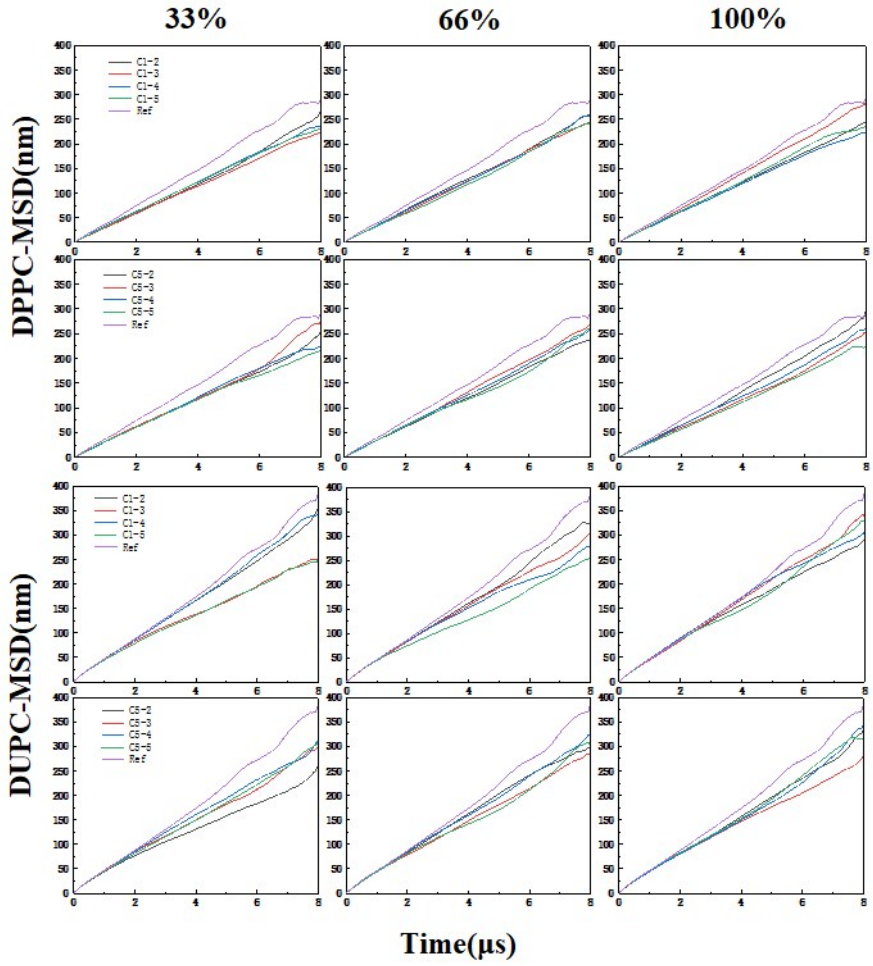

Figure S11. Time evolution of mean square displacement of saturated lipids and unsaturated lipids for NP-embedded lipid membrane systems (Ligand hydrophobicity: C1/C5, ligand length: nl=2, 3, 4, 5, ligand density: 33%, 66%, 100%) and the NP-free membrane system (Ref).

Table S1. The diffusion coefficients of saturated lipids (DPPC) and unsaturated lipids (DUPC).

DPPC	Diffusion coefficient		
(1e-5 cm^2/s)	33%	66%	100%
Ref	0.0383 (+/- 0.0037)		
C1-2	0.0313 (+/- 0.0075)	0.0312 (+/- 0.0000)	0.0297 (+/- 0.0006)
C1-3	0.0283 (+/- 0.0010)	0.0312 (+/- 0.0011)	0.0355 (+/- 0.0010)
C1-4	0.0297 (+/- 0.0006)	0.0304 (+/- 0.0008)	0.0287 (+/- 0.0014)
C1-5	0.0296 (+/- 0.0021)	0.0312 (+/- 0.0065)	0.0318 (+/- 0.0029)
C5-2	0.0281 (+/- 0.0001)	0.0298 (+/- 0.0018)	0.0351 (+/- 0.0034)
C5-3	0.0309 (+/- 0.0082)	0.0333 (+/- 0.0004)	0.0295 (+/- 0.0038)
C5-4	0.0297 (+/- 0.0014)	0.0315 (+/- 0.0027)	0.0313 (+/- 0.0030)
C5-5	0.0265 (+/- 0.0048)	0.0290 (+/- 0.0052)	0.0285 (+/- 0.0022)

DUPC	Diffusion coefficient		
(1e-5 cm^2/s)	33%	66%	100%
Ref	0.0463 (+/- 0.0075)		
C1-2	0.0405 (+/- 0.0018)	0.0405 (+/- 0.0070)	0.0344 (+/- 0.0053)
C1-3	0.0290 (+/- 0.0001)	0.0356 (+/- 0.0046)	0.0408 (+/- 0.0028)
C1-4	0.0428 (+/- 0.0062)	0.0313 (+/- 0.0090)	0.0381 (+/- 0.0094)
C1-5	0.0297 (+/- 0.0006)	0.0292 (+/- 0.0057)	0.0381 (+/- 0.0137)
C5-2	0.0271 (+/- 0.0029)	0.0386 (+/- 0.0027)	0.0380 (+/- 0.0020)
C5-3	0.0335 (+/- 0.0011)	0.0344 (+/- 0.0003)	0.0317 (+/- 0.0038)
C5-4	0.0363 (+/- 0.0038)	0.0383 (+/- 0.0023)	0.0379 (+/- 0.0088)
C5-5	0.0355 (+/- 0.0023)	0.0339 (+/- 0.0078)	0.0398 (+/- 0.0121)

6. Initial Configuration Influence on the Results.

In our work, the initial configuration of all our systems is the same with an NP embedded in the exact center of the lipid membrane. In order to understand whether the initial configuration has an impact on the final result, we changed the initial position of the nanoparticles and placed them away from the center of the membrane (**Fig. S12a**). It is showed that changing the initial position of the nanoparticles did not affect its ultimate targeting to lipid raft or non-lipid raft domains. Besides, the initial configuration with four NPs also reached the same conclusion, the number of nanoparticles did not affect its final localization (**Fig. S13**).

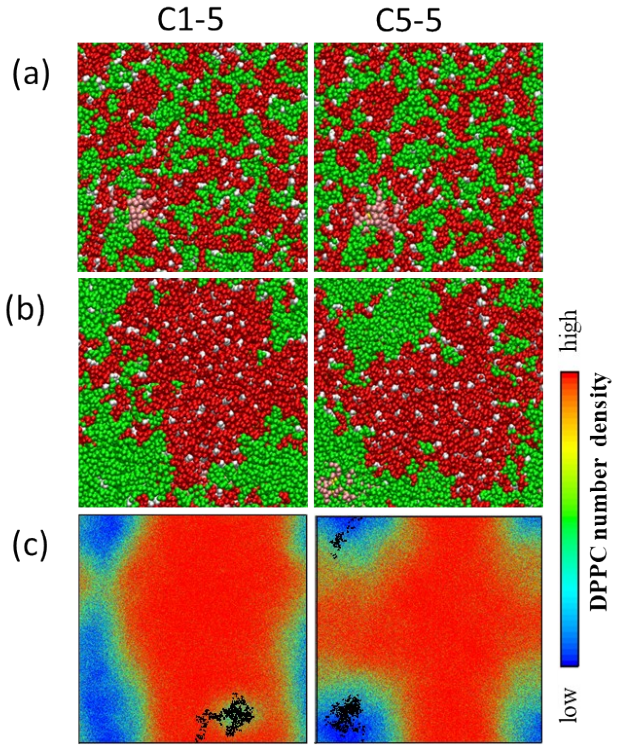

Figure S12. Effects of initial configuration on the membrane partitioning thermodynamics of ligand-modified NPs (ligand hydrophobicity: C1/C5, ligand density: 100%, ligand length: nl=5). **(a)** Initial configurations of the systems. **(b)** Top-view system snapshots of the last frame of each 8 μs trajectory. **(c)** 2D DPPC number-density maps and the location of NPs (black points) over each of the last 2 μs trajectories. The coloring style is the same as in **Fig. S4**..

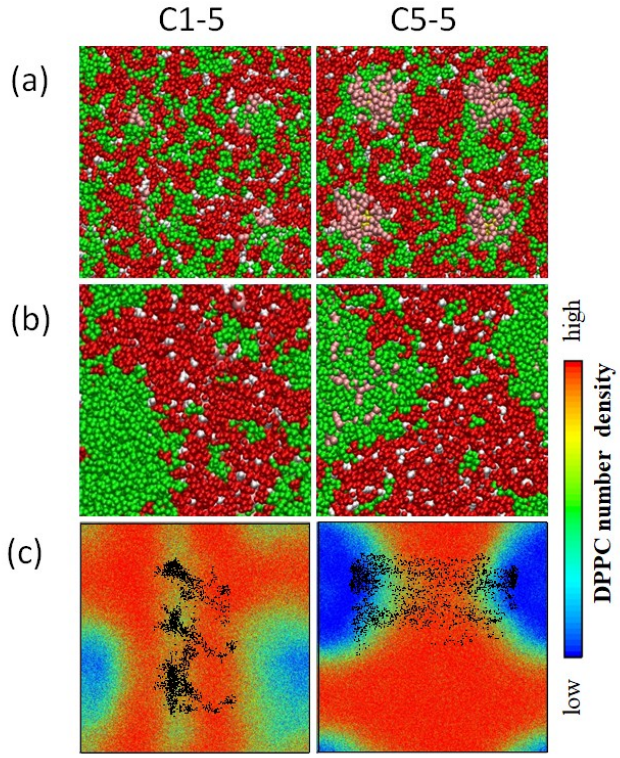

Figure S13. Effects of NPs' number on the membrane partitioning thermodynamics of ligand-modified NPs (ligand hydrophobicity: C1/C5, ligand density: 100%, ligand length: nl=5). **(a)** Initial configurations of the systems. **(b)** Top-view system snapshots of the last frame of each 8 μs trajectory. **(c)** 2D DPPC number-density maps and the location of NPs (black points) over each of the last 2 μs trajectories. The coloring style is the same as in **Fig. S4**.

7. Interactions between the different coarse grained (CG) beads in Martini force field.

In the manuscript, we have shown a series of quantitative analysis to reveal the roles of ligand hydrophobicity, length and density in NPs' preferred localization in the phase-separated lipid membranes. As for the exact molecular mechanism for different membrane partitioning thermodynamics, it can be ascribed to the nonbonded interactions between NPs and lipids/waters. NPs used here are neutral and hydrophobic. Hence, the nonbonded interactions are mainly Lennard-Jones (LJ) interactions. The interaction differences among C1, C5 and P5 are shown in Table S2. From the table, we can find that C1-type beads prefer C1-type beads more, and C5-type beads prefer C5-type beads more. These interaction differences induce different membrane portioning thermodynamics of ligand-modified NPs.

Table S2. The level of interactions between the different coarse grained (CG) beads in Martini force field.

	C1-C1	C5-C1	C5-C5	C1-P4	C5-P4	P4-P4
ε	3.5 kJ/mol	3.1 kJ/mol	3.5 kJ/mol	2.0 kJ/mol	3.1 kJ/mol	5.0 kJ/mol
σ	0.47nm	0.47nm	0.47nm	0.47nm	0.47nm	0.47nm

*water molecules use P4-type beads.